MAGNETIC AND DIELECTRIC PROPERTIES OF $CO_XZN_{1-X}FE_2O_4$ SYNTHESIZED BY METALLO-ORGANIC DECOMPOSITION TECHNIQUE

Anshu Sharma[1], Kusum Parmar[1], R.K. Kotnala[2] and N.S. Negi[1]
[1]Department of Physics, Himachal Pradesh University, Shimla, India
[2]National Physical Laboratory, New Delhi, India

ABSTRACT

Cobalt doped Zinc ferrites, $Co_xZn_{1-x}Fe_2O_4$, (x = 0, 0.2, 0.4, and 0.6) were prepared by chemical solution method using metallo-organic precursors. The crystalline structure, microstructure, magnetic and dielectric properties of the samples were investigated by X-ray diffraction (XRD), scanning electron microscopy (SEM), vibrating sample magnetometer (VSM) and impedance analyser respectively. All samples show cubic spinel structure with minor Fe_2O_3 phase and lattice parameter decreases from 8.419Å to 8.308Å with increasing cobalt content from 0 to 60%. Magnetic measurement shows that $Co_xZn_{1-x}Fe_2O_4$ samples exhibit ferromagnetic behavior at room temperature. The saturation magnetization initially increases from 2.17 to 71.2emu/g on increasing Co content to 40% and then decreases to value 55.9emu/g at Co concentration of 60%. The coercivity also increases to H_c ~ 330Oe for the sample with Co=20% and then decreases to minimum value of H_c ~ 32Oe for sample having 40% Co content. The coercivity value is then increases and is measured as H_c ~ 154Oe for sample with 60% Co content. The magnetic properties are explained in terms of cation distribution and grain size effect. The dielectric properties of the samples were studied with varying temperature and frequencies. The dielectric properties are influenced by electron hopping mechanism between Fe^{2+} and Fe^{3+} ions.

KEYWORDS: *Co-Zn Ferrite, MOD Technique, XRD, Magnetic properties, Dielectric properties*

I. INTRODUCTION

Ferrites continue to be a fascinating magnetic material because of their potential applications in high density information, ferro-fluids, magnetic resonance imaging, biomedical diagnostics, drug delivery, high frequency electronic devices, sensors, permanent magnets and magnetic refrigeration system etc [1-5]. Among various ferrites, $ZnFe_2O_4$ and $CoFe_2O_4$ have been most extensively studied systems, because they exhibit the typically normal and inverse spinel ferrites respectively [6,7]. Zinc ferrite bulk is antiferro magnetic below the Neel temperature (T_N = 10K) and turns to ferromagnetic or super paramagnetic when particle size reduces to a nanoscale. In $ZnFe_2O_4$, zinc ions occupy the tetrahedral sites and all Fe^{3+} ions occupy the octahedral sites. In contrast, $CoFe_2O_4$ exhibits ferromagnetism where cobalt ions occupy the octahedral sites and Fe^{3+} ions are equally distributed in tetrahedral and octahedral sites. Therefore, Co-Zn mixed ferrite has attracted considerable attention due to the completely different and interesting properties of $ZnFe_2O_4$ and $CoFe_2O_4$. Ferrites are usually prepared by autocatalytic decomposition [8], hydrothermal method [9-11], the reverse micelles method [12], co-precipitation [13], microwave combustion method [14] and sol-gel route [15]. The properties of the ferrites are highly sensitive to the ferrite compositions and synthesis techniques. S.B.Waje et.al [16]

prepared $Co_{0.5}Zn_{0.5}Fe_2O_4$ by mechanical alloying and sintering method. Dielectric studies of their specimen showed that permittivity remains constant with frequency and varies with the sintering temperature. Lopez et.al [17] recently synthesized Zn doped $CoFe_2O_4$ magnetic nanoparticles by using a co-precipitation method. They observed decrease in coercive field and particle size with the increase of Zn concentration. Hassadee et.al [18] reported decrease in the magnetization and the coercivity of Co-Zn ferrite with increasing zinc content due to the magnetic behavior and the anisotropic nature of cobalt. Gul et.al [19] investigated magnetic and electrical properties of $Co_{1-x}Zn_xFe_2O_4$ varying x from (0.0 to 0.6). A decrease in Curie temperature with an increasing Zinc doping concentration was observed. Temperature dependent dc resistivity measurements indicated semiconductor nature in Co-Zn ferrites. Veverka et.al [20] studied $Co_{1-x}Zn_xFe_2O_4$ around x=0.6 because of potential applications of the composition in the magnetic fluid hyperthermia. They reported that the cationic distribution in ferrite is more complex and the distribution is random in nature. They also observed that presence of vacancies in the octahedral sites changed the cobalt ions partially or completely to the Co^{3+} state. A neutron diffraction study showed the differences of cationic distributions in nanoparticles and bulk ferrite samples. On other hand, Ghasemi et.al [21] prepared $Zn_{1-x}Co_xFe_2O_4$ powder by sol-gel process and showed a transition from paramagnetic to ordered ferromagnetic state with increasing cobalt concentration. They also observed increasing behavior of saturation magnetization and coercivity of Co substituted $ZnFe_2O_4$ with an increase in cobalt content. Although, there have been considerable works mostly on $CoFe_2O_4$ side, systematic investigations of $Co_xZn_{1-x}Fe_2O_4$ system towards $ZnFe_2O_4$ are few and therefore an interesting subject to study.

In this work, we report the synthesis of $Co_xZn_{1-x}Fe_2O_4$ system with x = 0, 0.2, 0.4 and 0.6 by metal-organic decomposition (MOD) chemical route. To the best of our knowledge, no reports are available in the literature on studies of MOD processed Co-Zn ferrite. The advantages of this method include high solution stability, low processing temperature and composition is easily controllable. The structural, electrical and magnetic properties of $Co_xZn_{1-x}Fe_2O_4$ are systematically investigated.

II. EXPERIMENTAL

Cobalt Zinc mixed ferrite $Co_xZn_{1-x}Fe_2O_4$ where x = 0, 0.2, 0.4 and 0.6 were synthesized by chemical solution technique using metallo-organic precursors. In this method, Cobalt-2-ethyl hexanoate $(C_7H_{15}COO)_2Co$, Zinc-2-ethyl hexanoate $(C_7H_{15}COO)_2Zn$ and Iron-3-ethyl hexanoate $(C_7H_{15}COO)_3Fe$ were synthesized from starting materials $Co(NO_3)_2.6H_2O$, $Zn(NO_3)_2.H_2O$ and $Fe(NO_3)_3.9H_2O$ respectively. The $Co(NO_3).6H_2O$ was first dissolved in distilled water to prepare solution A. In a separate flask stoichiometric 2-ethyl hexanoic acid was neutralized by adding KOH solution under constant stirring to prepare solution B. The solution A was then poured into solution B under constant vigorous stirring. The Cobalt-2-ethyl hexanoate soap as formed was extracted with xylene solution. A clear solution of Cobalt-2-ethyl hexanoate in xylene was obtained and kept as cobalt stock solution. The chemical reactions during the synthesis can be represented as

1. $KOH + C_7H_{15}COOH \longrightarrow C_7H_{15}COOK + H_2O$

2. $2C_7H_{15}COOK + Co(NO_3)_2 \longrightarrow 2KNO_3 + (C_7H_{15}COO)_2Co$

Similarly, Zinc-2-ethyl hexanoate and Iron-3-ethyl hexanoate soaps were synthesized and extracted with xylene and kept as stock solutions for Zn and Fe respectively. The Chemical reactions are given below

3. $2C_7H_{15}COOK + Zn(NO_3)_2 \longrightarrow 2KNO_3 + (C_7H_{15}COO)_2Zn$

4. $3C_7H_{15}COOK + Fe(NO_3)_3 \longrightarrow 2KNO_3 + (C_7H_{15}COO)_3Fe$

These stock solutions were mixed in required molar ratio and magnetically stirred for 1hr at temperature ~70^0C. Polyethylene glycol (PEG) was added as surfactant. The resultant solution was subsequently dried at 300^0C. The dried powder was sintered at 700^0C for 3hr for crystallization. The powder was pressed into pallets by applying a load of about 5 ton and pallets were finally sintered at 1000^0C for 3hr in air.

The crystallographic and microstructure properties of the ferrites were studied by X-ray diffraction (PANalytical X'Pert PRO diffractometer) with CuKα radiation and scanning electron microscope (SEM) respectively. The compositional analysis of Co-Zn ferrites were performed using energy dispersive x-ray spectroscopy (EDXS). The dielectric measurements were performed by using Wayn Kerr 6520 impedance analyser in the frequency range of 20Hz to 1MHz. The magnetic properties were measured by using vibrating sample magnetometer VSM (Microsense, USA) at room temperature.

III. RESULTS AND DISCUSSION

Fig. 1 shows the XRD patterns of the MOD synthesized $Co_xZn_{1-x}Fe_2O_4$ (x = 0, 0.2, 0.4 and 0.6) powder sintered at 700^0C for 3hrs. All XRD peaks are indexed with the JCPDS Cards (# 22-1086 for $CoFe_2O_4$ and # 89-1012 for $ZnFe_2O_4$). The patterns show characteristic diffraction lines (220), (311), (222), (400), (422) and (511) of spinel cubic structure. The extra reflection peaks of Fe_2O_3 are also observed in XRD patterns of doped samples. The observation is not unusual particularly at a low sintering temperature. Tomer et.al [22] have also observed Fe_2O_3 impurity phase in Co-Zn ferrite powders synthesized by sol-gel process.

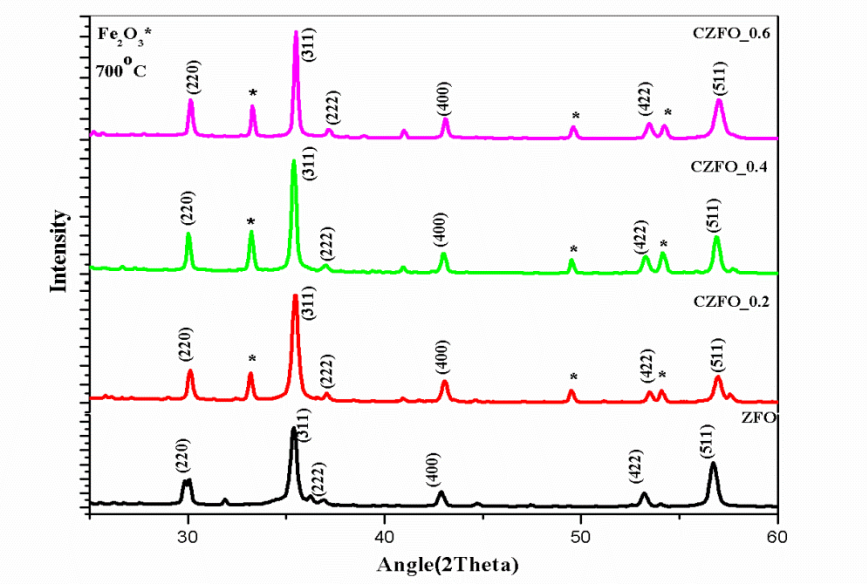

Fig.1 X-ray diffraction patterns for $Co_xZn_{1-x}Fe_2O_4$ (x = 0, 0.2, 0.4 and 0.6) samples sintered at 700^0C for 3hrs

Fig 2(a) shows all XRD patterns of the Co-Zn powders sintered at 1000^0C for 3hr. The absence of extra reflection peaks of Fe_2O_3 in the diffraction patterns of Co-Zn ferrite with x = 0 and 0.4 represents formation of single phase with a spinel crystal structure at the sintering temperature ~ 1000^0C. The Fe_2O_3 phase in other two samples with x = 0.2 and 0.6 is also significantly reduced on increasing sintering temperature. It can be seen from Fig.1 and 2(a) the degree of crystallinity of the samples increases on increasing sintering temperature from 700^0C to 1000^0C without any change in the basic crystal structure of Co-Zn ferrite. The lattice constant 'a' for each sample was calculated using relation $a = d(h^2+k^2+l^2)^{1/2}$ [23], where h,k,l are miller indices of the crystal planes. The dependence of the lattice parameter 'a' on Co^{2+} content is shown in fig.2(b). It can be seen that lattice constant 'a' of the samples decrease by increasing the sintering temperature from 700^0C to 1000^0C. This may be attributed to improvement in crystallization of the samples on increasing sintering temperature. On the other hand, the decrease in the lattice parameter 'a' with increasing Co concentration can be correlated with difference in ionic radii of Co^{2+} (0.78Å) and Zn^{2+} (0.82) [19] which means that more the Co^{2+} ion the less the lattice parameter. Fig. 2(b) also shows that the lattice parameter of Co-Zn ferrite decreases linearly with increasing Co concentration thus obeying Vegard's law approximately [24].

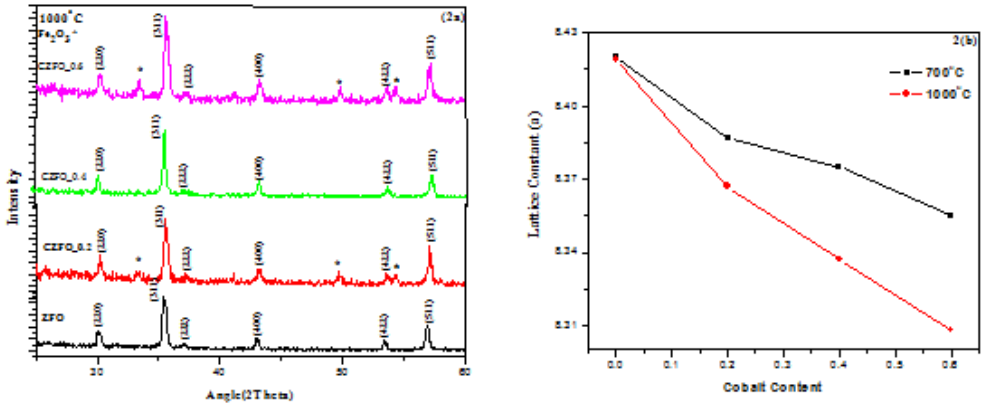

Fig.2 (a) X-ray diffraction patterns of $Co_xZn_{1-x}Fe_2O_4$ (x = 0, 0.2, 0.4 and 0.6) samples sintered at 1000^0C for 3hrs and (b) lattice constant of $Co_xZn_{1-x}Fe_2O_4$ (x = 0, 0.2, 0.4 and 0.6) samples with Cobalt concentration

The scanning electron microscope (SEM) images of Co-Zn ferrites sintered at 1000^0C are shown in Fig.3. In Fig.3 (a) to (d), it can be seen that particles are well distributed and agglomerated. Usually, these agglomerates are formed by smaller size particles. The size of the grain ranges from 95 to 142nm with varying Co concentration from 0 to 0.6. It is evident from Fig. 3(a) to (d) SEM images reveal dense microstructures.

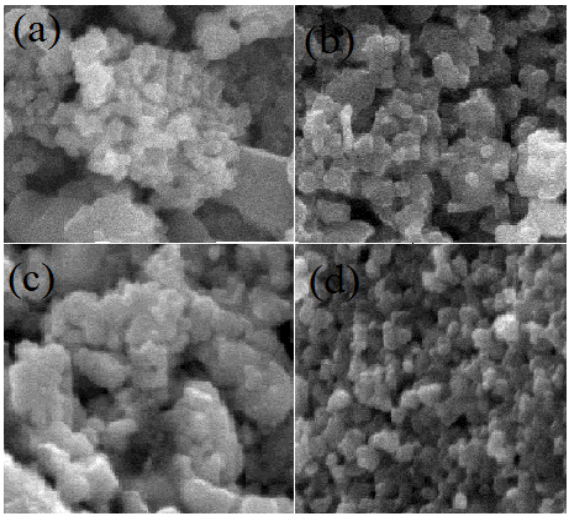

Fig.3 SEM micrographs of $Co_xZn_{1-x}Fe_2O_4$ (x = 0, 0.2, 0.4 and 0.6) samples

Energy dispersive x-ray spectroscopy (EDX) spectra of the samples sintered at 1000^0C are shown in Fig. 4(a) to (c). The presence of Co, Zn and Fe in the samples is depicted in the spectra. The EDX analysis indicates the wt% of cobalt and zinc in these samples are 9.55, 12.46, 17.41 and 9.32, 8.07. 4.67 respectively, which reveals the increasing concentration of cobalt and decreasing concentration of zinc in Co-Zn ferrite samples.

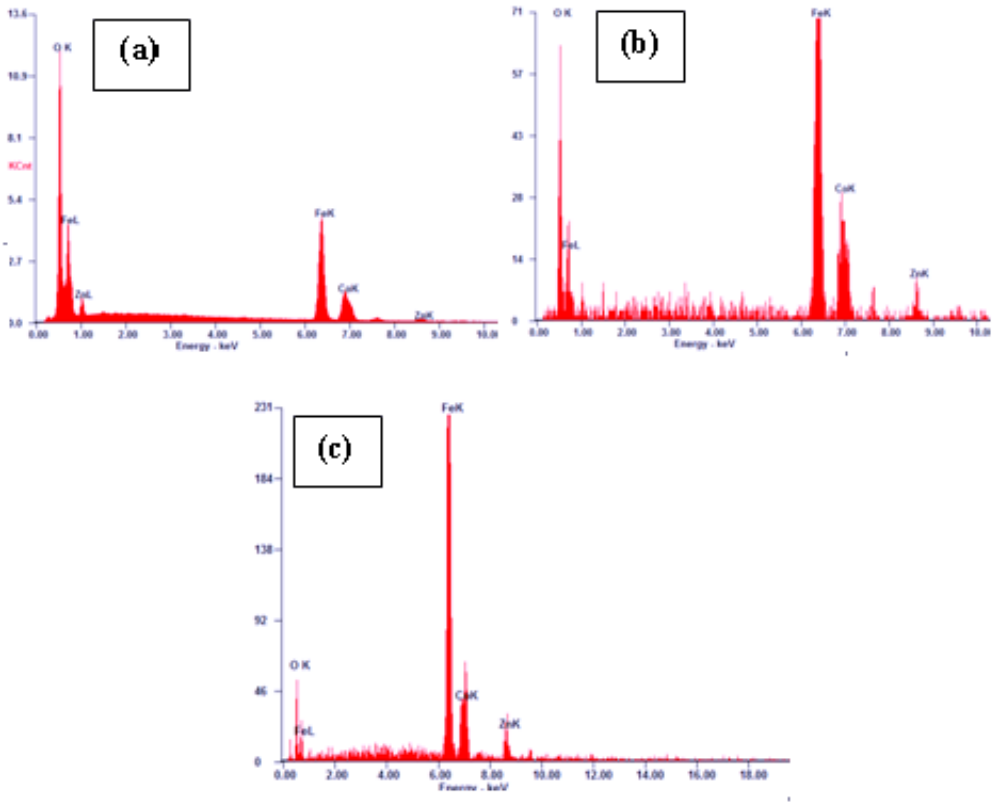

Fig.4 EDX of $Co_xZn_{1-x}Fe_2O_4$ (x = 0, 0.2, 0.4 and 0.6) samples.

Fig.5 shows the field dependent magnetization of $Co_xZn_{1-x}Fe_2O_4$ samples measured at room temperature in an applied field up to 20kOe. The magnetization increases with increase in external magnetic field strength at low field region and attains maximum value for field ~ 20kOe. It can be seen that all magnetization curves are saturated at higher field region and the hysteresis curves for samples are S shaped which are the characteristics of ferromagnetism.

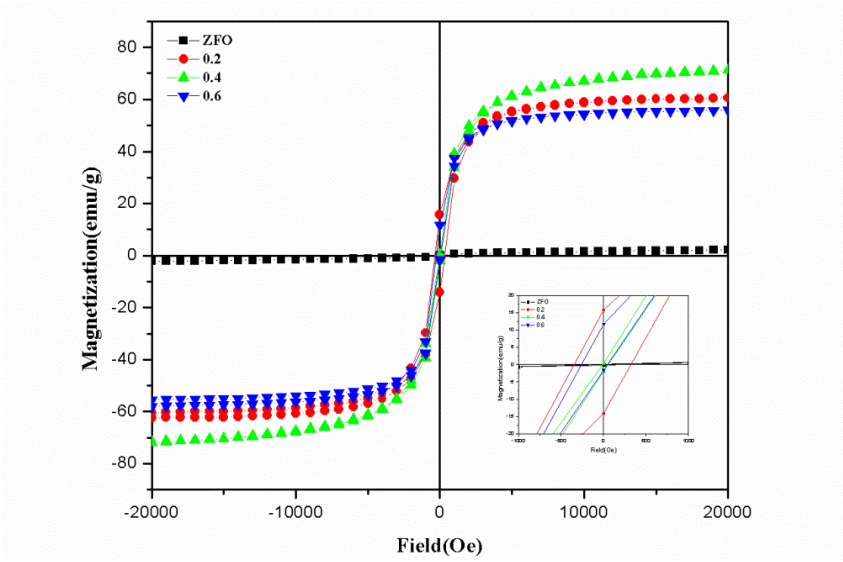

Fig.5 Magnetic hysteresis loops for $Co_xZn_{1-x}Fe_2O_4$ (x = 0, 0.2, 0.4 and 0.6) samples measured at room temperature.

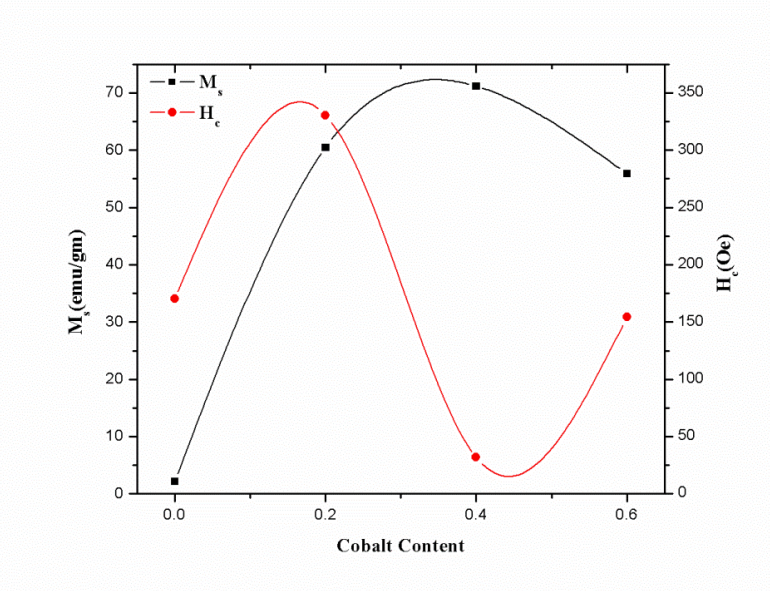

Fig.6 Variation of saturation magnetization and coercive field with Co concentration

Fig.6 shows the dependence of saturation magnetization M_s and H_c of the Co-Zn ferrite on Co content. In a cubic system of spinel ferrites the magnetic order is mainly constructed because of a super exchange interaction between metal ions of sub lattices A and B. The saturation magnetization first increases when cobalt content is between x = 0.0 and 0.4 and then decreases for x = 0.6. The increase in saturation magnetization is directly related to the enhancement in magnetic Co^{2+} ions replacing Zn^{2+} non magnetic ions, which affects the super exchange interaction [25,26]. The decrease in the saturation magnetization value for Co = 0.6 is due to the migration of Fe^{3+} ion from B site to A site, the magnetic moment of A site increases due to this net magnetization M_B-M_A decreases. As seen from Fig.6 with an increase in the Co^{2+} content coercivity H_c first increases for the samples with Co concentration with x = 0.2 and reaches minimum value H_c ~ 32Oe for x=0.4. It is then increased for x = 0.6. The increase in coercivity may be attributed to the increase in magnetocrystalline anisotropy with increasing Co content. The minimum value of H_c for x =0.4 may be attributed to its dominating minimum grain size effect (grain size ~95nm). It can be emphasized here that the observed values of M_s ~ 71.2emu/g and H_c ~ 32Oe for $Co_{0.4}Zn_{0.6}Fe_2O_4$ sample are significantly improvement over earlier reports [27-29]. The cation distribution formula for the mixed Co-Zn ferrite are given in Table I

Table I: Cation distribution in Co-Zn ferrites

Molecular formula	Cation distribution formula	
	[A-site]	[B-site]
$ZnFe_2O_4$	$[Zn^{2+}]$	$[Fe^{3+}]O_4$
$Zn_{0.8}Co_{0.2}Fe_2O_4$	$[Zn^{2+}_{0.8}Fe^{3+}_{0.2}]$	$[Co^{2+}_{0.2}Fe^{3+}_{1.8}]O_4$
$Zn_{0.6}Co_{0.4}Fe_2O_4$	$[Zn^{2+}_{0.6}Fe^{3+}_{0.4}]$	$[Co^{2+}_{0.4}Fe^{3+}_{1.6}]O_4$
$Zn_{0.4}Co_{0.6}Fe_2O_4$	$[Zn^{2+}_{0.4}Fe^{3+}_{0.6}]$	$[Co^{2+}_{0.6}Fe^{3+}_{1.4}]O_4$

Fig.7 (a) and (b) show variation of dielectric constant and dielectric loss (tanδ) with frequency at room temperature for Co substituted samples respectively. The dispersion in dielectric constant and loss tangent is observed in low frequency region for all samples. The dielectric constant decreases with increasing frequency.

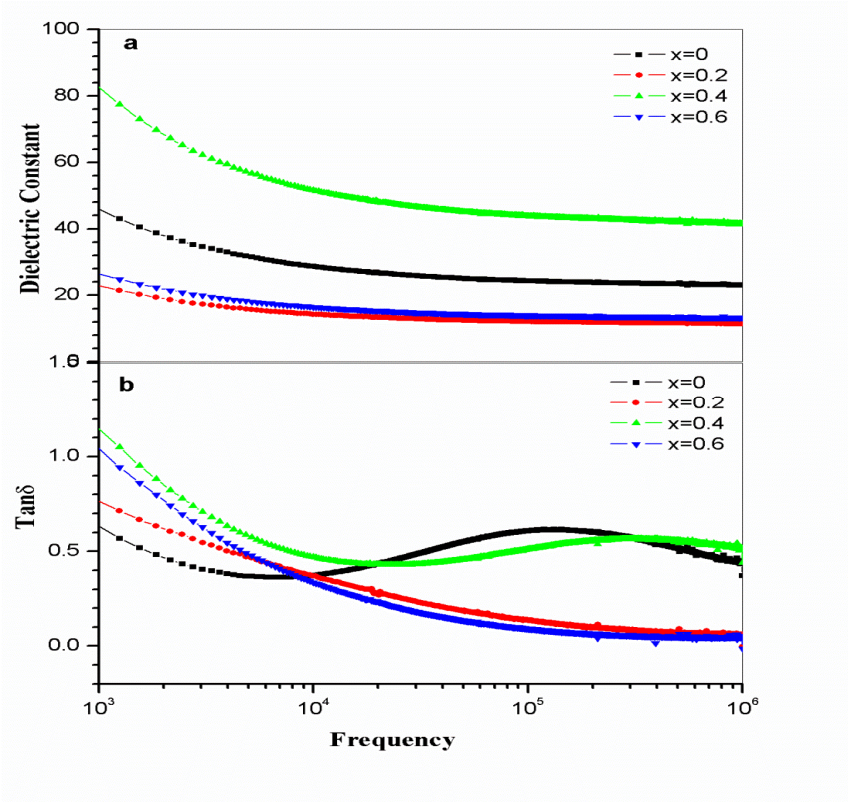

Fig.7 Variation in (a) dielectric constant (ε) and (b) dielectric loss (tanδ) with frequency at room temperature

The dielectric dispersion in Co-Zn ferrites can be explained on the basis of interfacial polarization as predicted by Maxwell-Wagner model. It is well known that dielectric structure of ferrite consists of conducting grains separated by the grain boundaries that are poor conductors. The hopping of electron between Fe^{2+} and Fe^{3+} results in the pile up of electrons at the grain boundaries and produce polarization in ferrites. However, as the frequency of the externally applied electric field is increased, the electron hopping between Fe^{2+} and Fe^{3+} does not follow the applied electric field as a result dielectric constant decreases and then becomes constant. The dielectric constant behavior is largely affected by Co content. The decrease in dielectric constant with increasing Co content for samples with x = 0.2 and 0.6 may be due to the migration of Fe^{3+} ions from octahedral site to tetrahedral site which decreases the hopping. However, the increase in dielectric constant for sample with x = 0.4 may be attributed to the formation of Fe^{2+} ions octahedral site. The formation of Fe^{2+} ions in octahedral site increases the electron exchange between Fe^{2+} and Fe^{3+} and hence enhances the polarization. The dielectric loss in ferrite mainly originates from electron hopping and defect dipoles. The electron hopping contributes to the dielectric loss only in low frequency range. The response of electron hopping is decreased with increasing frequency and hence the dielectric loss decreases in high frequency range as shown in fig.7(b). The charged defect dipoles contribute to the dielectric loss in high frequency range. In the meanwhile, dielectric loss peaks can be seen in fig.7(b) for sample with x = 0 and 0.4. For other two samples, the peaking behavior of dielectric loss is not observed in the measurable frequency range. The dielectric loss peak appears when the hopping frequency of the electron between Fe^{2+} and Fe^{3+} ions is close to the frequency of the external applied electric field. Furthermore, the loss peak in fig.7 (b) is moving to high frequency side with increase in Co content. This may be attributed to the fact that cobalt substitution prefers to the octahedral site which strengthens the dipole-dipole interaction that restricts the rotation of the dipoles.

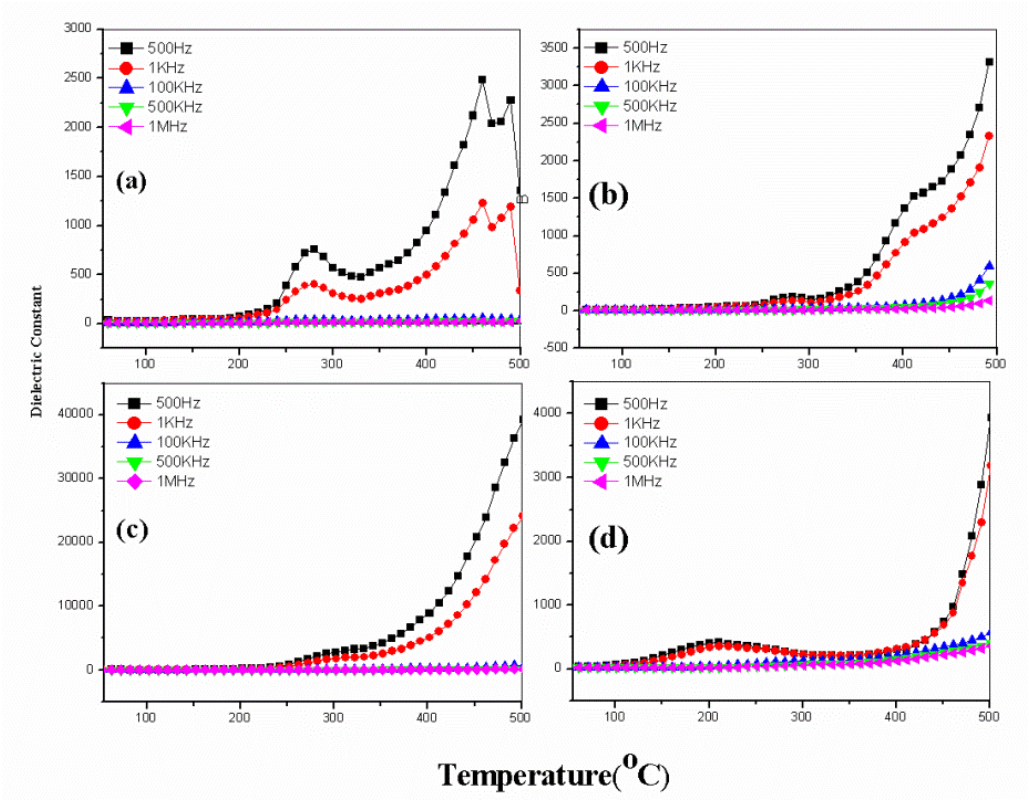

Fig.8 Temperature dependence of dielectric constant (ε) of $Co_xZn_{1-x}Fe_2O_4$ (x = 0, 0.2, 0.4 and 0.6) samples at different frequencies from 500Hz to 1MHz.

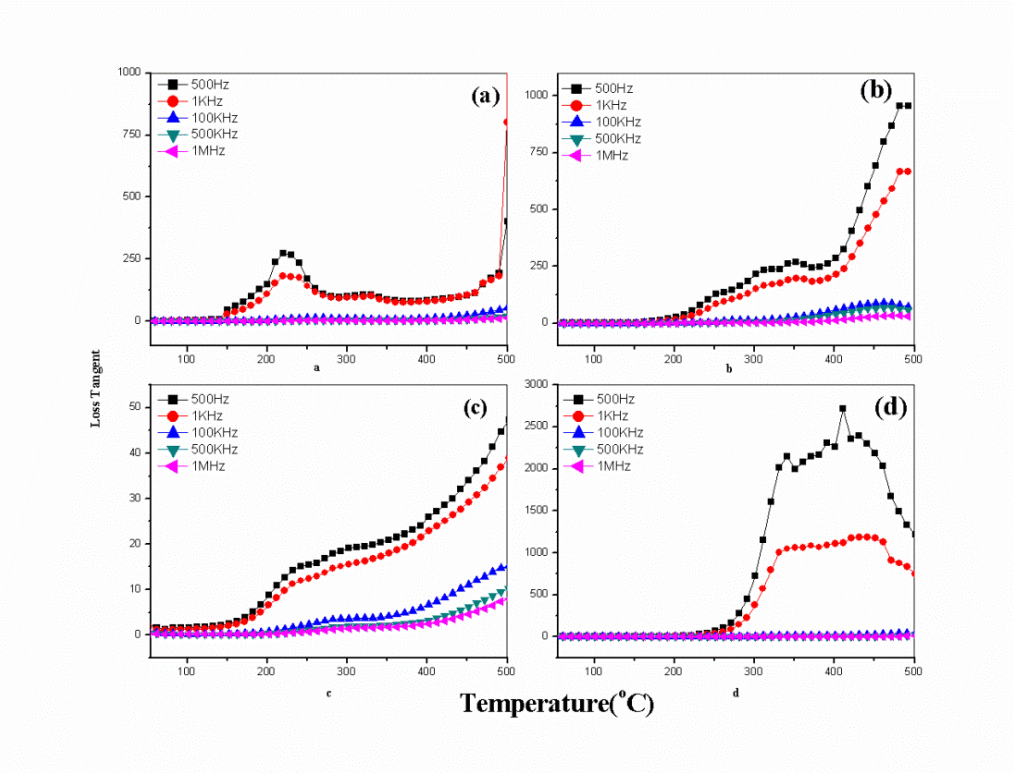

Fig. 9 Temperature dependence of dielectric loss (tanδ) of $Co_xZn_{1-x}Fe_2O_4$ (x = 0, 0.2, 0.4 and 0.6) samples at different frequencies from 500Hz to 1MHz

The temperature dependence of the dielectric constant and dielectric loss tangent measured at different frequencies 500Hz to 1MHz are shown in fig.8 and fig.9. It can be seen that all samples exhibit the frequency dependent phenomena which is attributed to the interfacial polarization in ferrite. It is noticed for all four samples that by increasing the temperature, the dielectric constant increases upto the specific maxima, which shift to higher temperature with increasing frequency. As the temperature increases more charge carriers get excitation from their trapping centers and contribute to the polarization. This in turn increases dielectric constant values of samples. The behavior of tanδ with Co content is similar to that of dielectric constant. Thermally activated dielectric behavior and conductivity give rise to tanδ > 1 at lower frequencies and high temperature [30].

IV. CONCLUSIONS

In conclusion Co substituted $ZnFe_2O_4$ systems have been successfully synthesized by chemical solution method using metallo-organic precursors. The XRD patterns revealed cubic spinel structure for all the compositions with minor impurity phase of Fe_2O_3 for samples with Co = 0.2 and 0.6 concentration. The lattice parameter decreases with increasing Co content due to smaller ionic radius of Co^{2+} than Zn^{2+} ion. SEM images showed fine-grained microstructures with grain sizes in the range of 95 to 142nm. The compositional analysis of these samples was performed by using EDX. As revealed by the observed results, the magnetic properties of the samples are mainly dominated by Co^{2+} ions replacing Zn^{2+} non magnetic ions as well as migration of Fe^{3+} ions from octahedral to tetrahedral sites. The cation distributions in mixed ferrites are very complex. The Mössbauer spectral study of the specimens is required to understand the magnetic properties completely and the investigation is under progress. The room temperature dielectric constant and loss tangent decrease with the increase in frequency indicates the normal dielectric behavior for all the samples. The variation of dielectric constant and loss tangent with temperature shows frequency dependent characteristics due to the electron hopping between the ions which plays dominant role in the dielectric behavior.

ACKNOWLEDGEMENT

One of the authors (Anshu Sharma) is very grateful to UGC, New Delhi for providing financial support under UGC-BSR fellowship.

REFERENCES

[1] Y.N. Xia et.al "One dimensional nanostructures: synthesis, characterization and applications" Adv. Mater. 15, 353 (2003)

[2] X. Kou et.al "Tunable ferromagnetic resonance in NiFe nanowires with strong magnetostatic interaction" Appl. Phys. Lett. 94, 112509 (2009)

[3] Q.A. Pankhurst, N.K.T. Thanh, S.K. Jones and J. Dobson, "Progress in applications of magnetic nanoparticles in biomedicine" J. Phys. D: Appl. Phys. 42, 224001 (2009)

[4] C.C. Berry, "Progress in functionalization of magnetic nanoparticles for applications in biomedicine" J. Phys. D: Appl. Phys. 42, 224003 (2009)

[5] Santosh Bhukal, Tsering Namgyal, S. Mor, S. Bansal and Sonal Singhal, "Structural, electrical, optical and magnetic properties of chromium substituted Co-Zn nanoferrites $Co_{0.6}Zn_{0.4}Cr_xFe_{2-x}O4$ ($0 \leq x \leq 1.0$) prepared via sol-gel auto-combustion method" J. Mol. Structure, 1012 (2012) 162-167.

[6] J.H. Shim, S. Lee, J.H. Park, S.J. Hau, Y.H. Jeong and Y.W. Cho, "Coexistence of ferromagnetic and antiferromagnetic ordering in Fe-inverted zinc ferrite investigated by NMR" Phys. Rev. B 73, 064404 (2006)

[7] T.M. Meaz, S.M. Attia and A.M. Abo El Ata, "Effect of tetravalent titanium ions substitution on the dielectric properties of Co–Zn ferrites" J. Magn. Magn. Mater. 210 (2000) 189

[8] L.R. Gonsalves, S.C. Mojumdar and V.M.S. Verenkar, "Synthesis and characterization of $Co_{0.8}Zn_{0.2}Fe_2O_4$ nanoparticles" J. Therm. Anal. Calorim. 104: 869-873 (2011)

[9] M. Sertkil, Y. Koseoglu, A. Baykal, H. Kavas and A.C. Basaran, "Synthesis and magnetic characterization of $Zn_{0.6}Ni_{0.4}Fe_2O_4$ nanoparticle via a polyethylene glycol-assisted hydrothermal route" J. Magn. Magn. Mater. 321, 157 (2009)

[10] F. Gozuak, Y. Koseoglu, A. Baykal and H. Kavas, "Synthesis and characterization of $Co_xZn_{1-x}Fe_2O_4$ magnetic nanoparticles via a PEG-assisted route" J. Magn. Magn. Mater. 321, 2170 (2009)

[11] H.Y. He, "Comparison study on magnetic property of $Co_{0.5}Zn_{0.5}Fe_2O_4$ powders by template-assisted sol-gel and hrdrothermal methods" J. Mater. Sci.: Mater Electron 23: 995-1000 (2012)

[12] V.L. Calero-Ddelc and C. Rinaldi, "Synthesis and magnetic characterization of cobalt-substituted ferrite ($CoxFe_{3-x}O_4$) nanoparticles" J. Magn. Magn. Mater. 314, 60 (2007)

[13] R. Arulmurugam, B. Jeyadevan, G. vaidyanathan and S. Sendhilnathan, "Effect of zinc substitution on Co-Zn and Mn-Zn ferrite nanoparticles prepared by co-precipitation" J. Magn. Magn. Mater. 288, 470 (2005)

[14] Y. Koseoglu, A. Baykal, F. Gozuak and H. Kavas, "Structural and magnetic properties of $Co_xZn_{1-x}Fe_2O_4$ nanocrystals synthesized by microwave method" Polyhedron 28, 2887 (2009)

[15] I. H. Gul and A. Maqsood, "Structural, magnetic and electrical properties of cobalt ferrites prepared by the sol–gel route" J. alloys Compd. 465, 227 (2008)

[16] S.B. waje, M. Hashim, W.D.W. Yusoff and Z. Abbas, "Sintering temperature dependence of room temperature magnetic and dielectric properties of $Co_{0.5}Zn_{0.5}Fe_2O_4$ prepared using mechanically alloyed nanoparticles" J. Magn. Magn. Mater. 322, 686 (2010)

[17] J. Lopez, L.F. Gonzalez-Bahamon, J. Prado, J.C. Caicedo, G. Zambrano, M.E. Gomez, J. Esteve and P. Prieto, "Study of magnetic and structural properties of ferrofluids based on cobalt-zinc ferrite nanoparticles" J. Magn. Magn. Mater. 324, 394 (2012)

[18] A. Hassadee, T. Jutarosaga and W. Onreabroy, "Effect of zinc substitution on structural and magnetic properties of cobalt ferrite" Procedia Engineering 32, 597 (2012)

[19] I.H. Gul, A.Z. Abbasi, F. Amin, M. Anis-Ur-Rehman and A. Maqsood, "Structural, magnetic and electrical properties of $Co_{1-x}Zn_xFe_2O_4$ synthesized by co-precipitation method" J. Magn. Magn. Mater. 311, 494 (2007)

[20] M. Veverka, Z. Jirak, O.Kaman, K. Knizek, M. Marysko, E. Pollert, K. Zaveta, A. Lancok, M. Dlouha and S. Vratislav, "Distribution of cations in nanosize and bulk Co-Zn ferrite" Nanotechnology, 22, 345701 (2011)

[21] A. Ghasemi, V. Sepelak, S.E. Shirsath, X. Liu and A. Morisako, "Mossbauer spectroscopy and magnetic characteristics of $Zn_{1-x}Co_xFe_2O_4$ (x = 0-1) nanoparticles" J. Appl. Phys. 109, 07A512 (2011)

[22] M.S. Tomar, S.P. Singh, O.P. Perez, R.P. Guzman, E. Calderon and C.R. Ramos, "Synthesis and magnetic behavior of nanostructured ferrites for spintronics" Microelectronic Journal 36, 475 (2005)

[23] Y.P. Fu and C.S. Hsu,"Microwave induced combustion synthesis of $Li_{0.5}Fe_{2.5-x}Mn_xO_4$ powder and their characterization" J. Alloys. Compd. 391, 185 (2005)

[24] A.R. Denton and N.W. Ashcroft, "Vegard's law" Phys. Rev. A 43, 3161 (1991)

[25] T. Ozkaya et.al, "Synthesis of Fe_3O_4 nanoparticles at 100^oC and its magnetic characterization" J. Alloys Compd. 472, 18 (2009)

[26] M. Sertkol et.al, "Microwave synthesis and characterization of Zn-doped nickel ferrite nanoparticles" J. Alloys Compd. 486, 325 (2009)

[27] S.U. Romero, O.P. Perez, O.N.C. Uwakwch, C. Osorio and H.A. Radovan, "Tunning of magnetic properties in Co-Zn ferrite nanocrystals synthesized by a size controlled co-precipitation method" J. Appl. Phys. 109, 07B512 (2011)

[28] S. Singhal, T. Namgyal, S. Bansal and K. Chandra, "Effect of Zn substitution on the magnetic properties of cobalt ferrite nano particles prepared via Sol-Gel route" J. Electromagnetic Analysis & Applications, 2, 376 (2010)

[29] R. Rani, S.K. Sharma, K.R. Pirota, M. Knobel, S. Thakur and M. Singh, "Effect of zinc concentration on the magnetic properties of cobalt–zinc nanoferrite" Ceramic International 38, 2389 (2012)

[30] C. Harnagea, L. Mitoseriu, V. Buscaglia, I. Pallecchi and P. Nanni, "Magnetic and ferroelectric domain structures in $BaTiO_3$–$(Ni_{0.5}Zn_{0.5})Fe_2O_4$ multiferroic ceramics" J. Eur. Ceram. Soc. 27, 3947 (2007)

AUTHORS

Anshu Sharma is pursuing Ph.D from Himachal Pradesh University, Shimla. She did her M.Sc. and M.Phil degrees in the years 2006 and 2007. She has attended three international and three national conferences/workshops and presented papers. Her area of research focused on magnetic materials and composite materials

Kusum Parmar has obtained her M.Sc. degree in 2007 and M.Phil degree in 2009 in Physics from Himachal Pradesh University, Shimla and has joined Ph.D from the same university. She has attended four national conferences and workshops. Her area of research interests are ferrite/ferroelectric composite materials and thin film.

R. K. Kotnala obtained Ph.D. degree from Indian Institute of Technology, Delhi in1982. At present working as a chief scientist at National Physical Laboratory, New Delhi, India and he is Fellow IGU. His current field of interest is, multiferroics, magnetic materials, magnetic standards and sensor materials inclusive of nanomagnetism of materials.

N. S. Negi joined the Himachal Pradesh University, Shimla in October 1997. He received his PhD degree from the Himachal Pradesh University Shimla. He has extensive experience in deposition of ferroelectric & ferrite thin films. He currently works on ferroelectric & multiferroic thin films, high k materials, diluted magnetic semiconductors & pyrophoric materials. He has published over 40 papers in international journals. Currently he is a Professor and Head, Department of Physics. H.P. University, Shimla.

.